2017 INTERNATIONAL OIL SPILL CONFERENCE

The Direct Quantitative Measurement of In-Situ Burn (ISB) Rate and Efficiency

Paul D. Panetta[1,2], Richard Byrne[1], and Hualong Du[1]

[1]Applied Research Associates, Inc., Route 1208 Greate Road, Gloucester Point, VA 23062;

[2]Virginia Institute of Marine Science of the College of William & Mary, Gloucester Point, VA 23187-8795

ABSTRACT

In-situ burning (ISB) is an important tool to remove oil from the environment. During ISB, it is important to know the volume reduction of oil for the overall accounting of the spilled oil, as a metric for operational decisions, and to account for the ISB portion of the oil budget. The burn rate depends on the type of oil, degree of emulsification and weathering, estimated thickness, weather conditions, and size of the burn area. Furthermore, each spill has a unique physical environment and oil properties that affect burn efficiency and rate. The volume of oil consumed during ISB is typically computed using a manual, coarse, time integration of the instantaneous burn area based on visual observations and a characteristic burn rate. The area is typically estimated in the field using known boom geometry and visual inspection of the fire-water interface, and recorded manually.

We have developed methods to measure the instantaneous consumption of burning oil and thus the oil burn rate by integrating direct measurements of thickness using acoustics sensors in the water under the slick with direct measurements of the area of the burning oil using infrared and visible light images from cameras above the burning oil. Data were collected during the burning of several oils and petroleum products including ANS, rock, diesel, and hexane. The acoustic thickness measurement took into account the high temperature gradient in the oil and

combined with multi camera automated burn area estimates yielded an instantaneous measurement of the volume of oil consumed while burning.

We were able to identify the buildup of the burn, the active burning phase, and in the case of confined burns the vigorous burning phase. Knowing the instantaneous thickness and surface area during burning allowed us to directly calculate the burn rate and to study the dynamics of ISB. We are working on validating the burn rate and efficiency with direct measurements of the weight of the oil and residue before, during, and after burning. The authors believe these are the first direct measurements of slick thickness using acoustics during ISB.

INTRODUCTION

In-situ burning (ISB) is an important tool used by spill responders to remove oil from the environment [Alan and Ferek]. During burn operations, it is important to know the volume reduction of oil for the overall accounting of the spilled oil, as a metric of success of various remediation methods, and to account for the ISB portion of the oil budget [Lehr et al]. The burn rate (volume/time) depends on the type of oil, emulsification, estimated thickness, and size of the burn area. The area is typically estimated in the field using known boom geometry and visual inspection of the fire-water interface [Allen et al., Fingas (2014), Fingas (1999), S.L.Ross]. This manual process is extremely labor intensive and time consuming. In addition, each spill has a unique physical environment and set of oil properties that consequently affects burn efficiency and burn rate. In the lab, burn efficiency is determined by calculating the difference between the initial mass of oil and the mass of the residue divided by the initial mass of oil. While very effective in the lab, measurements of the initial and residual masses of oil in real spill

environments are not feasible. We developed tools to quantify the efficiency and rate of burning in real time.

METHODS

Acoustic measurement of thickness

The ability to measure the slick thickness with acoustic measurements hinges on the ability to measure the reflection from the oil-water interface. The strength of the reflection from the oil water interface is controlled by the difference of acoustic impedances of the water and the oil. The acoustic impedance is $Z = \rho V$, where ρ is the density of the fluid and V is the speed of sound. The reflection coefficient, R, is given by the following equation.

$$R = \frac{Z_{water} - Z_{oil}}{Z_{water} + Z_{oil}}$$

If the acoustic impedances of the water and oil are equal, then there will be no reflection from the water oil surface. For the oils and temperatures used for this study R ranged from ~0.15 at room temperature to ≳0.3 during burning.

The acoustic signals from the oil slick is shown in Figure 1 along with a schematic of the measurement sensor and slick. The data on the right side shows the reflections from bottom of the slick, the top of the slick, and a reverberation inside the slick. The thickness was calculated from the difference in the arrival between the bottom and top of the slick.

It is important to note that the speed of sound in the oil changes with temperature and that the temperature varies dramatically from the bottom of the slick, which is in contact with the water, to the top of the slick, which is in contact with the burning oil vapor. To accurately determine the thickness, we measured the speed of sound of several oils over from ~ 25°C to 180°C as shown in

Figure 2. The speed of sound in oil is directly related to viscosity, which decreases as temperature increases, accounting for the decrease in the speed of sound as the temperature increased.

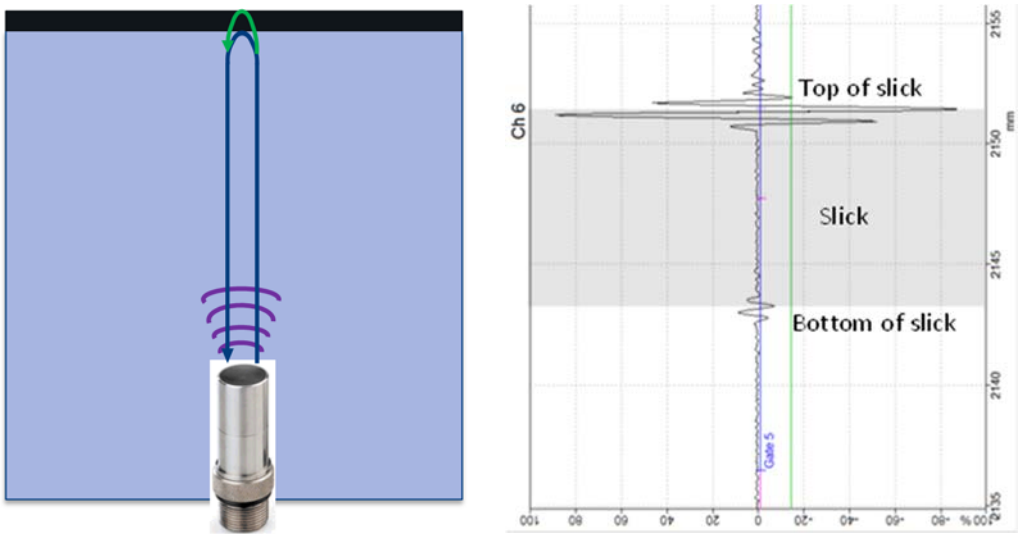

Figure 1. Schematic of acoustic measurements of slick thickness and accompanying data.

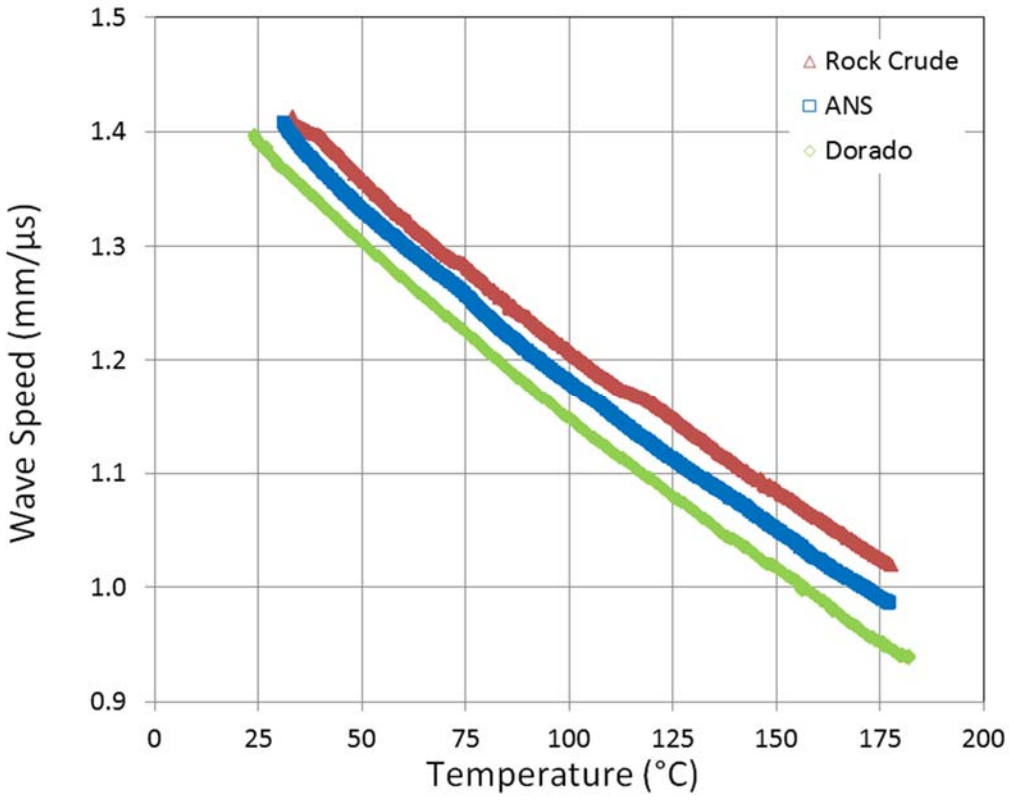

Figure 2. Acoustic speed of sound of various crude oils as a function of temperature.

Measurement of surface area

The development of the burn area estimate and its validation in the lab has taken into consideration the open water burning scenario. The burn area estimate was designed to require two or more cameras which can capture some or all of the burn region. These cameras can be at a low vantage point as if they were on the deck of a ship or an aerial vantage point like a UAV.

The algorithm used all available imagery of the fire and transformed them into a 'birds eye view' reference frame using a planar homography [Kanatani]. This top down view, is better than the side perspective for tallying geometry since the area of pixels has a proportional relation to burn area. An example of transforming images using a planar homography is shown in Figure 3. With actual fire the images from multiple perspectives were transformed immediately and then superimposed to find the area. The time to do the computation changes with the number of cameras and their resolutions occurs in the order of a few seconds.

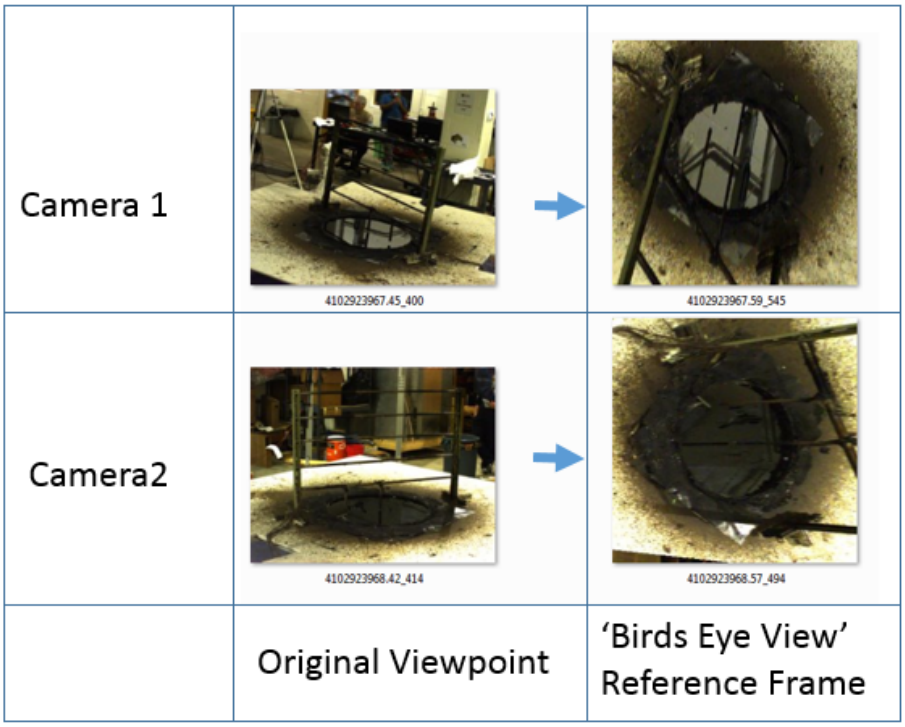

Figure 3. Image processing to convert side view of images to bird's eye view.

As an example Figure 4 shows the fire from 3 of the 6 visible light cameras used in the measurements. Notice that in last image on the right there is an area free of burning. Notice the right side of the center image also shows part of the non-burning area with some of it obscured by the flames. Figure 5 shows the same three images transformed to the birds eye view and rotated to be in the same horizontal plane coordinate system.

Figure 4. Side view of burning ANS

Figure 5. Transformed bird's eye view of burning ANS

Using image processing techniques such as dilation, blurring and thresholding, the red, green, and blue (RGB) values for the visible light cameras show the interior of the fire can determined as shown in Figure 6 and Figure 7.

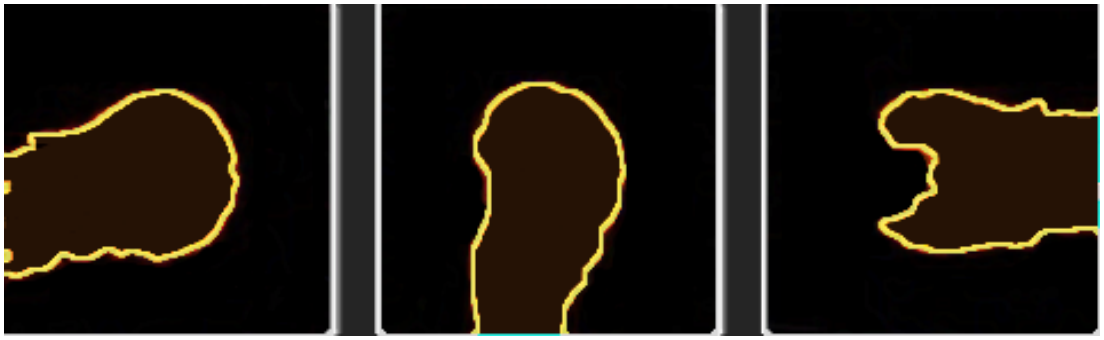

Figure 6. The interior of the fire after processing from 3 cameras.

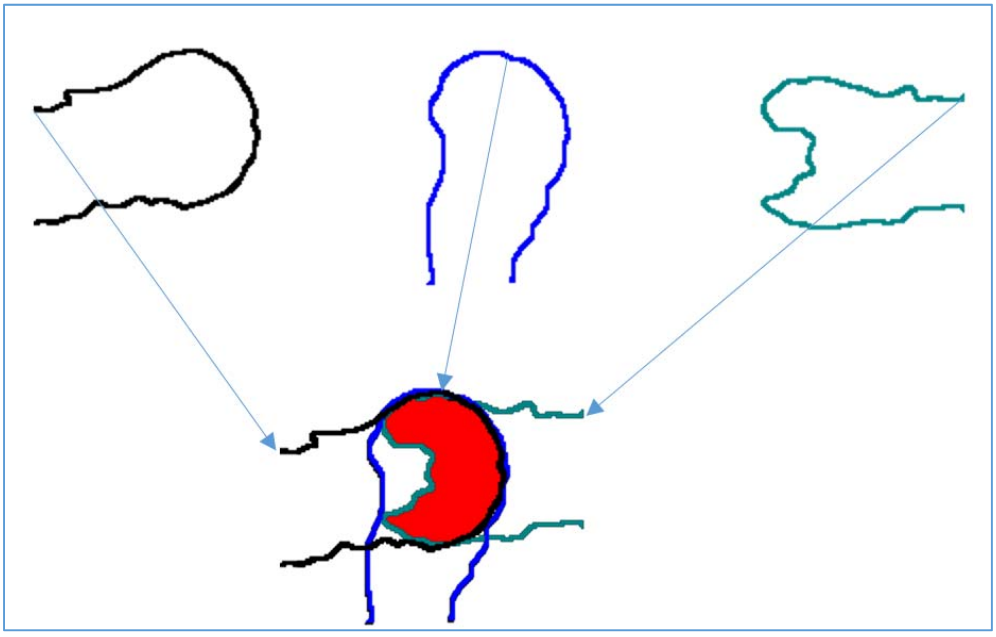

Figure 7. The resultant fire calculated from 3 different cameras.

In this reference frame the fire area is combined to yield a burn area, Figure 7, shown in red. The process described here given the setup during our measurements using six 1024 x 768 cameras takes less than 2 seconds. The process to determine the homography in the lab is done with fixed coordinates determined ahead of time and once the matrix is constructed the actual transformation is instantaneous. There are two methods to be used in the field. One uses common points found in the captured imagery to co-register the 'birds eye view' imagery and the other can use GPS coordinates and pose associated with each camera to formulate the transform.

Experimental Setup

Thermocouples and acoustic transducers were mounted on a frame inside a tank as shown in Figure 8 to allow data collection during burning. The 16 thermocouples were separated by 1 mm vertically and the thermocouple tree was adjusted for each burn to enable the temperature profile in the slick to be measured. Several visible and IR cameras were placed around the burn apparatus in protective cases as shown in Figure 8. The 70 cm diameter tank was filled with water approximately 5 cm above the transducers and oil was poured to create a slick of approximately 1 cm thick. The initial volume of oil was approximately 3.8 L.

Figure 8: Acoustic transducers and thermocouples mounted inside the 70 cm diameter burn chamber and the camera enclosure.

RESULTS AND DISCUSSION

Direct Measurement of Oil Thickness and Temperature During ISB

Acoustic data was collected during the burning of several oils and petroleum products including ANS, rock, diesel fuel, and hexane. For this work we will report on burning ANS to

show the methods and results. The acoustic signals from one of the sensors below the burning oil are shown in Figure 9. The vertical axis is the distance the acoustic wave travels in the oil slick and the horizontal axis is the time during the burn. Each vertical line is an individual acoustic signal similar to the one shown in Figure 1 with the color representing the amplitude of the signal (black is low and red is high). The horizontal lines from 0 seconds until ~ 40 seconds are the signals from the bottom of the slick, the top of the slick, and multiple reverberations inside the slick before the oil was ignited. After the oil was ignited the acoustic signals from the bottom and the top of the slick were still visible. We use the difference between those two signals to calculate the thickness during the burn. Evident in this sonar-like image is the high degree of returned signal, or scattered signal, at and above the top of the oil slick. The scatter is caused by the boil over of the liquids which occurs almost immediately for the oil and at ~ 200 seconds into the burn for the water as indicated by the scatter and movement of the bottom of the slick starting at about 240 seconds into data collection. The vigorous burning phase can be seen to occur from ~225 seconds through 350 seconds as indicated by the high degree of scattering and large amplitude signals in that time frame.

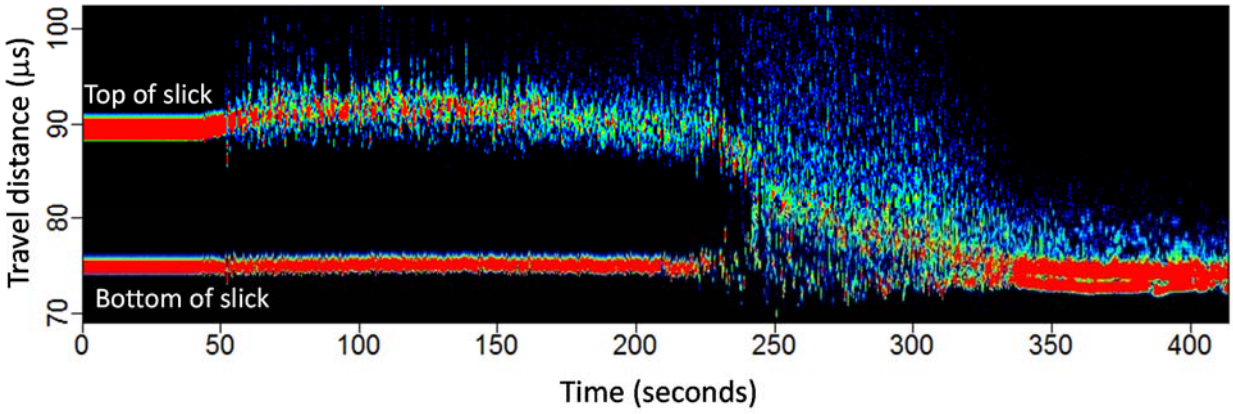

Figure 9. Sonar-like acoustic image showing the reflections from the slick surfaces during ISB.

To determine the instantaneous thickness, we accounted for the change in the speed of sound as a function of the temperature using the data shown in Figure 2. The resultant temperature profiles in the oil slick are shown in Figure 10. The depth and time dependence are along the vertical and horizontal lines are shown in the

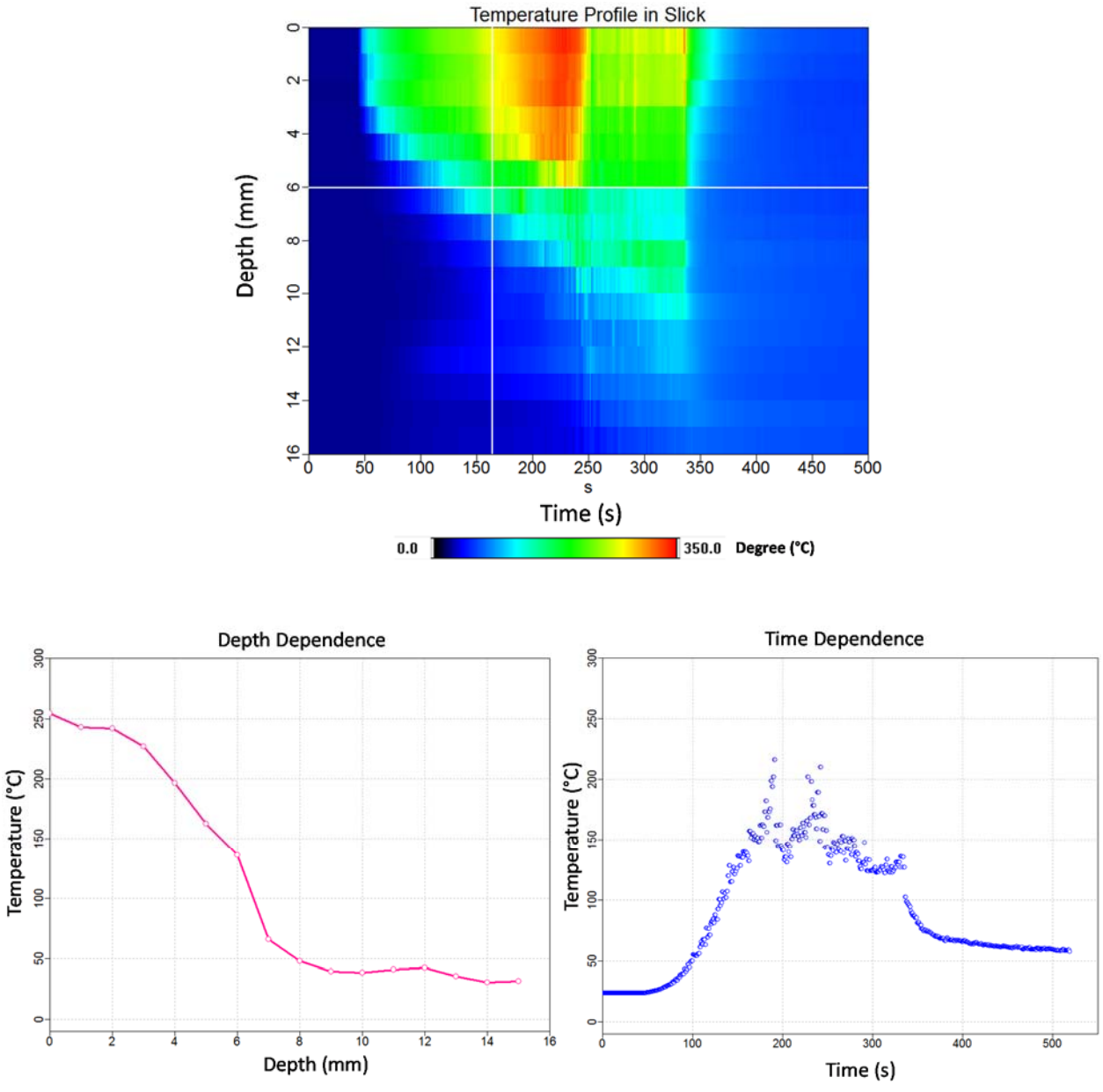

Figure 10. Temperature measurements inside the slick (top) as afunction of depth (bottom left), and as a fucntion of time 6 mm below the surface of the slick (bottom right).

The measurement of the temperature inside the slick was used to calculate the instantaneous speed of sound and thus the thickness during burning as shown in Figure 11. The oil was ignited approximately 40 seconds after data collection started. The thickness appeared to initially increase from 10.2 mm to ~ 10.8 mm. This initial increase could be related to the fact that the thermocouples and the acoustic sensors were not in the exact same location and thus significant temperature gradients may have existed affecting our temperature correction to the speed of sound. After approximate 100 seconds, the thickness decreased rapidly. After 200 seconds the oil began to vigorously burn and boil over accelerating the decrease in the thickness of the slick. The decrease in the thickness then slowed down until the fire extinguished at about 340 seconds. We can identify several regions of the burning including the initial phase where the flames cover the oil surface, then steady burning after 100 seconds where the oil consumption increased. The vigorous burning phase is evident in the rapid decrease in the thickness followed by slower consumption until the flame out. The authors believe these are the first measurements of the thickness of an oil slick using acoustics during burning.

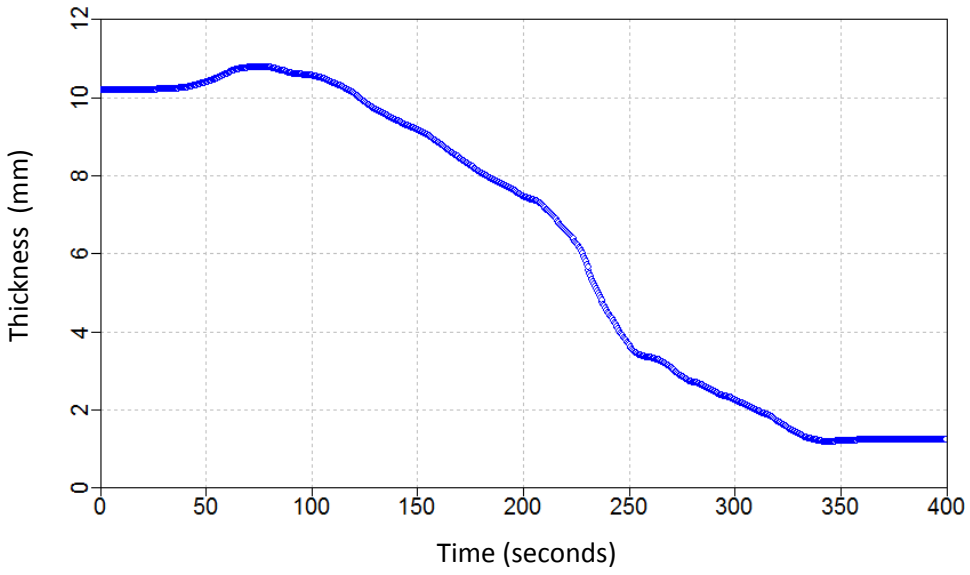

Figure 11. The instantons measurement of slick thickness during burning using acoustics.

Direct Measurement of Surface Area of Burning Oil

Using the methods described above, the instantaneous surface area was computed as a percentage of full tank area as shown in Figure 12. The surface area of the burning oil increased to nearly 100% nearly immediately after ignition, fluctuated around ~90%, then remained at 100% until the fire began to burn down.

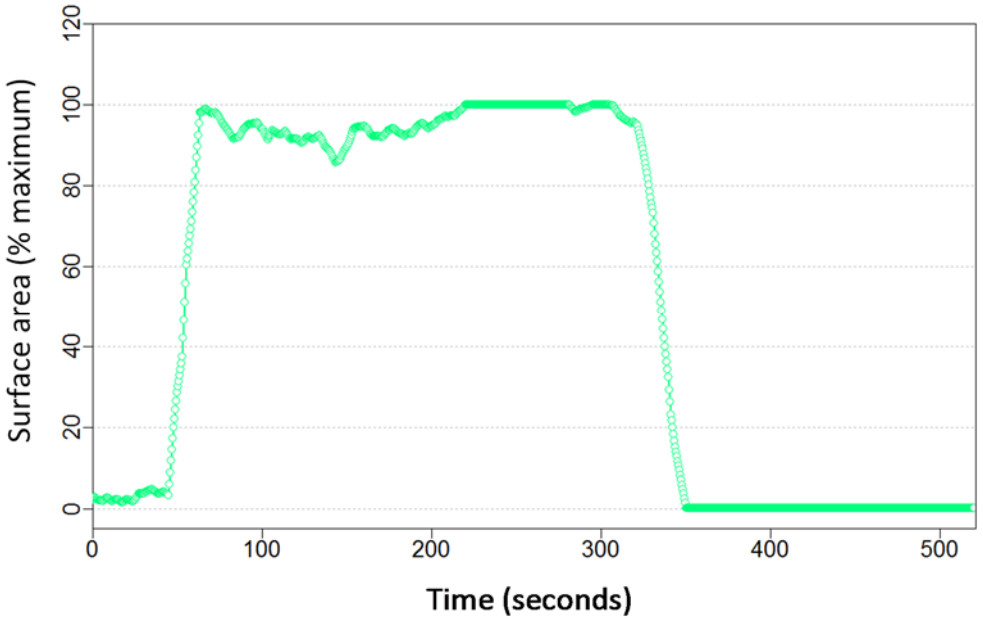

Figure 12. The surface area calculated during the burning of ANS.

In-situ Measurement of Oil Consumption and Instantaneous Burn Rate

By combining the instantaneous measurement of slick thickness from acoustics with surface area from the visible images we were able to calculate the instantaneous volume of oil consumed during the burning process. To calculate the volume during the burn required a two-step process, first the temperature profile was measured during a burn, then the calculation of the speed of sound as a function of time during the next burn was calculated. Four stages of burning

can be identified. The initial stage where the oil began to burn during the first 100 seconds after measurements began (note that the oil was ignited using a propane torch approximately 40 seconds after measurements began. During the next stage the consumption rate was steady until the vigorous boiling phase where the consumption rate increased dramatically, followed by a burn down phase before flame out. Based on these data we calculated the efficiency of this burn to be ~ 90%, which is similar to previously reported numbers for similar oils [Fingas, Merv (2014)]. In future work we will compare these efficiency measurements with direct measurements of the oil mass before and after burning.

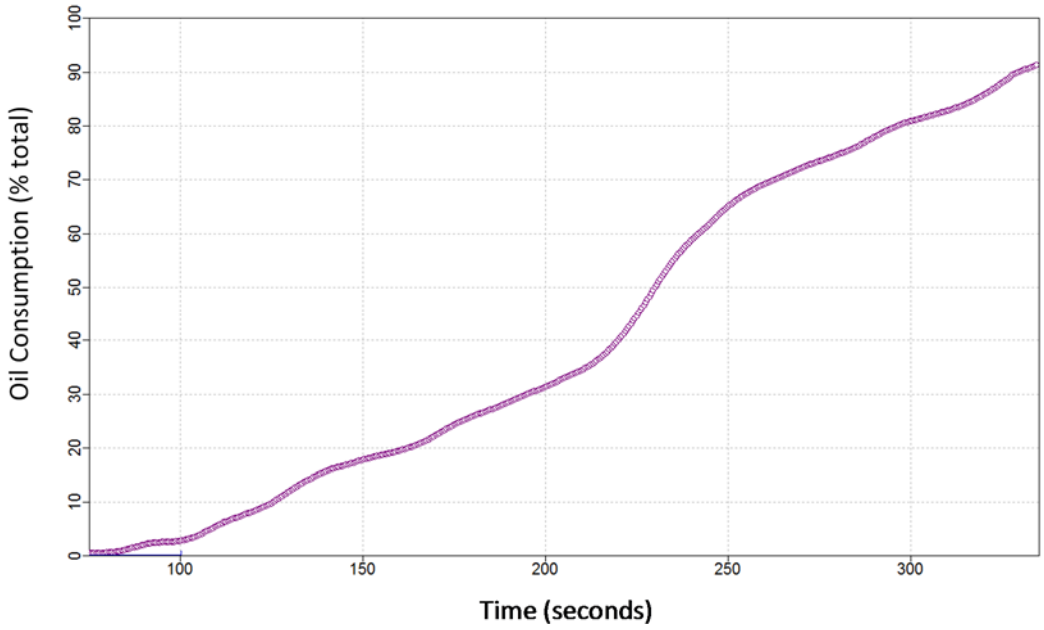

Figure 13. The instantaneous consumption of oil based on direct measurements of slick thickness and surface area.

Using the oil consumption vs. time we calculated the instantaneous burn rate by calculating the slope of the oil consumption over a 10 second moving window as shown in Figure 14. The phases of burning can be seen in the burn rate vs time graph with the initial rate ramping up then oscillating around 10 cm^3/s followed by the vigorous boiling phase where the rate increased to ~ 40 cm^3/s then decreased rapidly back to near 10 cm^3/s to 15 cm^3/s until flame

out. These values are in line with previously published work on similar oils [Fingas, Merv (2014)]. We are in the process of benchmarking these preliminary measurements with direct measurements of the weight loss of oil during burning and the weight of the oil and residue. We will report those results in the future.

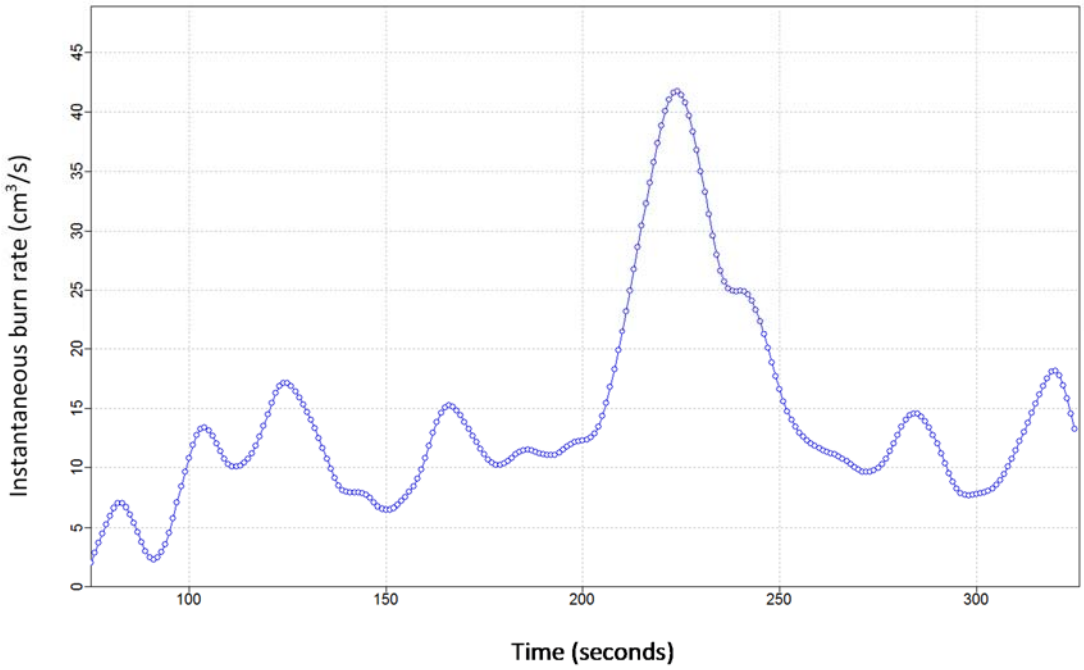

Figure 14. The instantaneous burn rate calculated from the in-situ measurement of thickness an surface area (10 cm^3/s = 0.6 L/min).

CONCLUSIONS

We developed measurements to quantify burn rate and efficiency instantaneously during ISB using acoustic measurements of slick thickness and imaging measurements of the surface area. We are working on benchmarking these results with direct measurements of the weight of oil before, during and after burning. Future work will include measurements performed in ice fields as well as work with herders and ROV deployments of the acoustic measurements. These

techniques offer unprecedented ability to study the dynamics of burning oil and to calculate the burn rate during ISB.

REFERENCES

Allen, Alan A., and Ronald J. Ferek. "Advantages and disadvantages of burning spilled oil." International Oil Spill Conference. Vol. 1993. No. 1. American Petroleum Institute, 1993.

Allen, Alan A., et al. "The use of controlled burning during the Gulf of Mexico Deepwater Horizon MC-252 oil spill response." International Oil Spill Conference Proceedings (IOSC). Vol. 2011. No. 1. American Petroleum Institute, 2011.

Fingas, M.F (1999) "In situ burning of oil spills: a historical perspective." NIST SPECIAL PUBLICATION SP (1999): 55-66.

Fingas, Merv (2014) “In-situ Burning of Oil”, February 2014.
Kanatani, K. Guide to 3D Vision Computation: Geometric Analysis and Implementation. Cham, Springer International Publishing, 2016.

Lehr, B., S. Nristol, and A. Possolo. "Oil Budget Calculator”, Deepwater Horizon, Technical Documentation: A Report to the National Incident Command." Federal Interagency Solutions Group, 2010.

S.L.Ross (1999), “Laboratory Testing to Determine In Situ Burning Parameters for Six Additional U.S. OCS Crude Oils”, 1999.

ACKNOWLEDGMENTS

This study was funded by the Bureau of Safety and Environmental Enforcement (BSEE), U.S. Department of the Interior, Washington, D.C., under Contract No. E15PC00005. The authors would like to especially thank Professor Ali Rangwala, Dr. Kemal Arsava, and their team for their work setting of and conducting the burns at the Worcester Polytechnic Institute.